JACS
JOURNAL OF THE AMERICAN CHEMICAL SOCIETY
pubs.acs.org/JACS
Communication

Full Visible Spectrum and White Light Emission with a Single, Input-Tunable Organic Fluorophore

Andrés Zavaleta,* Aleksandr O. Lykhin, Jorge H. S. K. Monteiro, Shoto Uchida, Thomas W. Bell, Ana de Bettencourt-Dias, Sergey A. Varganov, and Judith Gallucci

Cite This: J. Am. Chem. Soc. 2020, 142, 20306−20312
Read Online

ABSTRACT: The blue emission of M2biQ can be tuned to specific wavelengths throughout the visible region by changing the identity of the cation it interacts with. These optical properties are observed in MeCN solution and the solid state. White light is obtained in MeCN by using either the proper ratio of zinc ions or acid. Thus, M2biQ acts as a nearly universal emitter (λ_{em} = 468−690 nm) with large Stokes shifts (116−306 nm, $\Delta\tilde{\nu}$ = 7,042−11,823 cm^{-1}). Full spectral profiles as well as quantum yields, lifetimes, and the crystal structures of key RGB and yellow emitters are reported. Emission wavelengths correlate with cationic radius, and TD-DFT calculations show that, for 1:1 complexes, the smaller the ion, the shorter the N−cation bond, and the greater the bathochromic emission shift.

The development of a single tunable fluorescent dye with a wide emission range is of interest for simplifying the fabrication of multicolor optoelectronic devices, such as organic light-emitting diodes (OLEDs).[1−9] Obtaining emissions that encompass the full spectrum typically requires the use of numerous fluorescent molecules[7−15] or quantum dots,[16,17] each one covering a particular portion of the spectrum. Metal binding,[4,18−25] protonation,[2,25−27] organic supramolecular interactions,[1,4,28−37] manipulation of aggregation or solid-state structure,[5,7,38−47] solvatochromic effects,[14,15,48−52] isomerizations,[53−55] and variable labeling of biomolecules,[56] among other methods,[32,42,50,55,57,58] have also been pursued to introduce further color variations. Here we report our unexpected discovery of the outstanding intrinsic photoluminescence of 6,7-dihydro-1,12-dimethoxydibenzo-[*b*,*j*][1,10]phenanthroline[59] (Figure 1), otherwise known as dimethoxydimethylenebiquinoline (M2biQ). Upon cation binding, this simple fluorophore exhibits differential red-green-blue (RGB) luminescence that was previously thought possible only by using entire arrays of ion sensors.[22,30] It also provides intermediate colors without the need of mixing different dyes or chelates,[37,54] or the need to adjust the ratio of the metal ion guest to the sensor.[18,28]

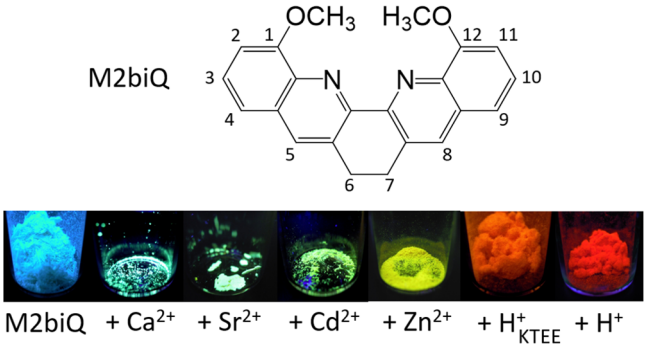

Figure 1. Structure of M2biQ and solid-state fluorescence (λ_{ex} = 365 nm) of the free ligand and some of its salts. All samples were isolated from wet acetonitrile except for H^+_{KTEE}, which was isolated from KOH/TFA/EtOH/Ether (KTEE). All other counterions are ClO_4^-. See pp S66, 72 for details.

M2biQ was prepared by a Friedländer condensation[60] between 2-amino-3-methoxybenzaldehyde[61] and 1,2-cyclohexanedione (see p S2). The blue fluorescence of M2biQ can be selectively red-shifted by simply adding the proper main group or transition metal ion or acid (Figures 1 and 2), thus making fluorescence-tuning a straightforward task.

Single crystal X-ray structures corresponding to RGB and yellow emitters are shown in Figure 3. Electronic repulsion between the lone pairs of the pyridine N atoms prevents the two methoxyquinoline halves of free M2biQ from being coplanar while the dimethylene bridge (dihedral angle $C_{Ar}C_6-C_7C_{Ar}$ = 53.9°) preorganizes the ligand for metal-ion binding. Cation binding reduces the dihedral angles (NC−CN and ω) for the 1:1 complexes in the progression M2biQ·Ca^{2+} > M2biQ·Zn^{2+} > M2biQ·H^+ (Table 1). Because the difference in twist angles from species to species is small, and the same yellow emission was observed for M2biQ$_2$·Zn^{2+} and M2biQ·Zn^{2+} species with different degrees of planarization, the increasingly red-shifted emissions are attributed to the decreasing N−cation distances (N−Ca^{2+} (2.5 Å) > N−Zn^{2+} (2.1 Å) > N−H^+ (0.9 Å)). This correlation involving shorter N−metal bonds and longer emission wavelengths is also seen

Received: July 29, 2020
Published: November 17, 2020

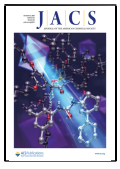

https://dx.doi.org/10.1021/jacs.0c08182
J. Am. Chem. Soc. 2020, 142, 20306−20312

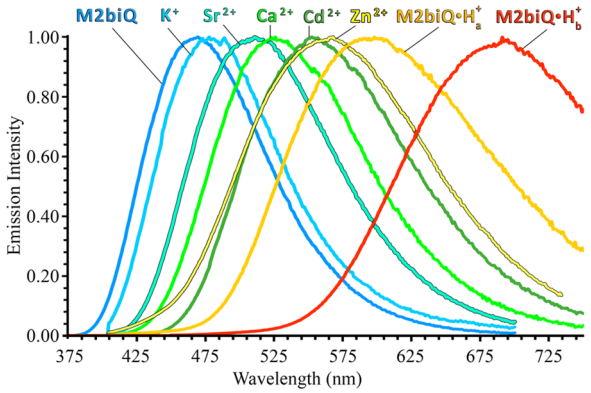

Figure 2. Normalized emission spectra of M2biQ and its complexes (10^{-4} M) in MeCN. Salts used: KSCN, $Sr(ClO_4)_2$, $Ca(ClO_4)_2$, $Cd(NO_3)_2$, and $Zn(ClO_4)_2$. H_a^+ = TFA/MeCN (1:4, v/v) and H_b^+ = HCl (generated *in situ*). See pp S32–S33, for details.

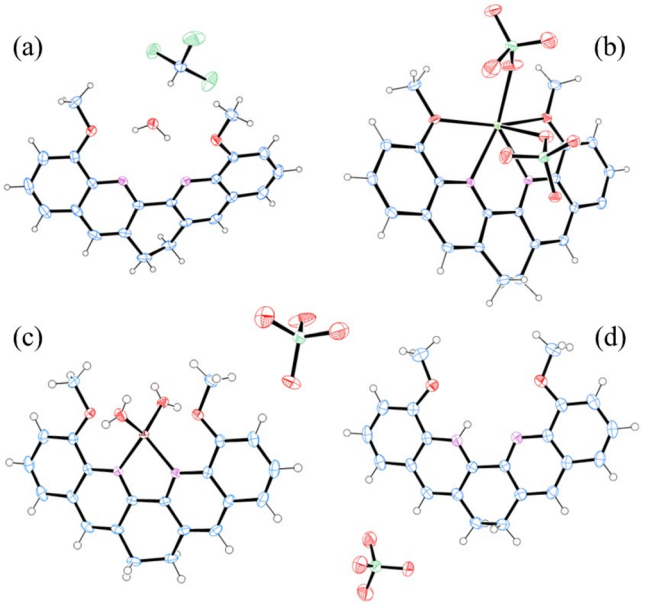

Figure 3. Solid-state structures of RGB and yellow emitters. (a) Blue emitter: M2biQ·H_2O·$CHCl_3$, (b) green emitter: M2biQ·$Ca(ClO_4)_2$, (c) yellow emitter: M2biQ·$Zn(ClO_4)_2$·$2H_2O$, and (d) red emitter: M2biQ·$HClO_4$·H_2O. C atoms (blue), O atoms (red), N atoms (violet), Cl atoms (green), Zn atom (purple), Ca atom (light green). See pp S208–S209 for the M2biQ$_2$Zn^{2+} encapsulating complexes (pairs 1 and 2).

with 8-hydroxyquinoline (8-HQ), the parent compound of M2biQ.[62] The shorter N–cation bonds also correlate, as expected, with the relative ionic radii of the ions (Ca^{2+}(1.14 Å) > Zn^{2+} (0.88 Å) > H^+).

The λ_{max} values for the absorption and emission bands of free M2biQ, its protonated form, and complexes with potassium, strontium, calcium, cadmium, and zinc were determined in acetonitrile (Table 2). Very large Stokes

Table 2. Experimental and Calculated (c) Absorption and Emission Wavelengths (λ_{max}, nm) of M2biQ Species in Acetonitrile ([M2biQ] = 10^{-4} M)

Species[a]	λ_{abs}	λ_{abs} (c)	λ_{abs}	λ_{abs} (c)	λ_{em}	λ_{em} (c)
M2biQ	276	294	352	331	468	456
M2biQ·K^+	276	290	356	342	477	458
M2biQ·Sr^{2+}	273	287	366	353	510	485
M2biQ·Ca^{2+}	279	288	367	359	528	489
M2biQ·Cd^{2+}	282	293	368	362	551	514
M2biQ$_2$·Zn^{2+}	288	303	376	369	581	558
M2biQ·H^+	290	304	384	380	690	585

[a]Salts used: KSCN, $Sr(ClO_4)_2$, $Ca(ClO_4)_2$, $Cd(NO_3)_2$, and $Zn(ClO_4)_2$, or TFMS as the acid. Counterions used in calculations are consistent with salts, except for counterion-free M2biQ$_2$·Zn^{2+}. All other complexes were assigned a 1:1 stoichiometry for calculations.

shifts[63,64] ranging from 116 to 306 nm ($\Delta\tilde{\nu}$ = 7042 to 11 823 cm^{-1}) were observed. The spectra were obtained by mixing solutions of M2biQ with the metal salts or by generating HCl *in situ* or by adding trifluoromethanesulfonic acid, TFMS (see Supporting Information). Binding constants (Table S1) for the complexes corresponding to the crystal structures were found from UV–visible titrations[65] (see Figures S13, S15, S21): Ca^{2+} K_{11} = 1.0 × 10^{12}, K_{21} = 1.0 × 10^{20}; Zn^{2+} K_{11} = 3.3 × 10^8, K_{21} = 2.7 × 10^{19}, and H^+ K_{11} = 1.9 × 10^4. Speciation diagrams[66] show that, as the equivalents of Ca^{2+} gradually increase from 0.5 to 1.0, M2biQ$_2$·Ca^{2+} converts to M2biQ·Ca^{2+}. In contrast, M2biQ$_2$·Zn^{2+} is the dominant complex at all concentrations, so wavelengths are given for this species in Table 2. The most obvious trend in Table 2 is the order of increasing emission wavelength: M2biQ < M2biQ·K^+ < M2biQ·Sr^{2+} < M2biQ·Ca^{2+} < M2biQ·Cd^{2+} < M2biQ$_2$·Zn^{2+} < M2biQ·H^+. The λ_{abs} values show similar, but less pronounced trends.

Our orange crystals (H^+_{KTEE}, Figure 1), isolated from KOH/TFA/EtOH/Et_2O (KTEE), were too small for crystallographic characterization. We, therefore, provisionally assume they are monoprotonated and attribute their different color to polymorphism.[5,40,42,44,67] The orange emission of M2biQ·H_a^+

Table 1. Bond Lengths[a] and Dihedral Angles NC–CN and ω in Single Crystal X-ray Structures Corresponding to RGB and Yellow Species

Crystal	Bond Length/Å N–Guest	Bond Length (Å) O–Guest	Dihedral angle NC–CN (ω)[b]
M2biQ·H_2O	2.46/2.53 (N---H_2O)	2.15/2.20 (O---H_2O)	23.8° (24.3°)
M2biQ·Ca^{2+}	2.46/2.47 (N–Ca^{2+})	2.50/2.51 (O–Ca^{2+})	9.0° (10.4°)
M2biQ·Zn^{2+}	2.05/2.05 (N–Zn^{2+})	2.62/2.62 (O–Zn^{2+})	8.1° (10.2°)
M2biQ·H^+	0.86 (N–H^+)	2.31 (O---H^+)	7.5° (7.9°)
M2biQ$_2$·Zn^{2+}	2.04/2.04 (N–Zn^{2+})	2.71/2.71 (O–Zn^{2+})	7.1° (11.2°)
(pair 1)	2.06/2.06 (N–Zn^{2+})	2.74/2.74 (O–Zn^{2+})	14.0° (12.6°)
M2biQ$_2$·Zn^{2+}	2.06/2.06 (N–Zn^{2+})	2.76/2.77 (O–Zn^{2+})	16.5° (19.6°)
(pair 2)	2.04/2.04 (N–Zn^{2+})	2.67/2.78 (O–Zn^{2+})	16.0° (18.8°)

[a]The dotted lines (---) represent hydrogen bonds. [b]ω is the angle between the two pyridine planes (see p S167).

https://dx.doi.org/10.1021/jacs.0c08182
J. Am. Chem. Soc. 2020, 142, 20306–20312

(Figure 2), where M2biQ is assumed to be in a particular protonation state, was obtained by using a mixture of TFA in MeCN. Solvatochromism[14,15,51,52] also seems to be in operation (see pp S63–64). Without the methoxy groups, the emission in MeCN only reaches 430 nm (λ_{ex} = 250 nm) upon addition of $HClO_4$.[68] Related cation-sensitive push–pull single-molecule emitters, whose structure also remains intact upon ion binding, exhibit a narrower multicolor spectral profile and/or require the use of toxic metal ions (Hg^{2+}, Cd^{2+}, Pb^{2+}) to generate key colors.[2,19,25,52]

Selected photophysical data[69−71] for the RGB and yellow emitters are shown in Table 3. These appeared to be

Table 3. Quantum Yields and Lifetimes for RGB and Yellow Emitters in Acetonitrile[a]

Substance	Quantum yield, φ	Reference Standard	Lifetime τ (/ns)
M2biQ	0.25	Quinine sulfate[69,70]	5.55 ± 0.03
M2biQ·Ca^{2+}	0.44	Fluorescein[70,71]	17.3 ± 0.01
M2biQ$_2$·Zn^{2+}	0.01	$Ru(bpy)_3Cl_2$[70,71]	6.88 ± 0.03
M2biQ·H^+	0.001	$Ru(bpy)_3Cl_2$[70,71]	Unable to measure

[a]Counterion: $CF_3SO_3^-$. For details, see S83–S163.

photostable upon prolonged standing under ambient light and/or irradiation at 1, 30, and 60 min. The quantum yield (QY) of M2biQ is similar to that of 8-methoxyquinoline.[72] The higher QY upon Ca^{2+} binding is likely due to increased conformational restriction of the receptor[73] as suggested by a reduced nonradiative/radiative transitions ratio (k_{nr}/k_r) with respect to free M2biQ (see pp S83–84). With the smaller Zn^{2+} and H^+ ions, the MeO groups can be free to participate in an $n-\pi^*$ fluorescence-quenching charge-transfer process to the heterocyclic core.[25,74] The ability of bipyridines to act as electron acceptors when bound to Zn^{2+} and H^+ ions is well documented.[75,76] This may explain the low QY for these complexes. Also, deactivation by proton transfer[77] or solvent relaxation[78] appears to be particularly in operation with the protonated complex (see p S72). As expected, our Zn^{2+} and protonated complexes appear much brighter in the solid state. Additionally, by using the proper amount of acid or Zn^{2+} in MeCN, it is possible to obtain warm, cool, or nearly pure white light[79,80] (see pp S17–20, 28–30).

Computational studies were performed using the time-dependent density functional theory (TD-DFT) at the B3LYP/def2-SVP level with the SMD solvation model to account for the solvation effects of acetonitrile (see p S167). The DFT-predicted geometries reveal that UV-excitations of M2biQ, its protonated forms, and 1:1 metal complexes are accompanied by contraction of the twist angle ω between the quinoline rings in the excited states, while photon emission is followed by expansion of ω in the ground state. For example, for M2biQ, the ground S_0 and emitting S_1 states are characterized by ω = 18.2° (∠NC–CN = 18.5°) and ω = 15.8° (∠NC–CN = 9.1°), respectively. Such photoinduced planarization is known for other fluorophores,[81,82] but those metal-free compounds display larger dihedral angle changes (≥16°). In the M2biQ metal complexes, the relative twisting in the emitting state with respect to the ground state gradually decreases from $\Delta\omega$ = 2.7° in M2biQ·K^+ to $\Delta\omega$ = 0.3° in M2biQ·Zn^{2+}. Thus, metal binding reduces the conformational differences between the ground and emitting states.

The frontier molecular orbitals of M2biQ and the key electronic transitions are shown in Figure 4. The prominent

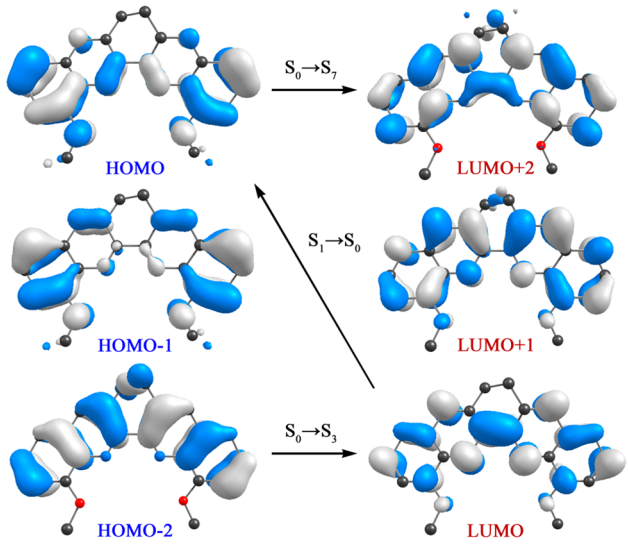

Figure 4. M2biQ frontier molecular orbitals at the equilibrium geometry of the ground state.

absorption band observed at 276 nm can be attributed to $S_0 \rightarrow S_7$(HOMO → LUMO+2) excitation, and the second broad band at 352 nm is likely due to collective excitations $S_0 \rightarrow S_1$(HOMO → LUMO), $S_0 \rightarrow S_2$(HOMO−1 → LUMO), and $S_0 \rightarrow S_3$(HOMO−2 → LUMO); the latter has the largest oscillator strength. Since the HOMO and HOMO−2 have a nodal plane across the central NC–CN bond, electrons in these orbitals reduce the NC–CN bond order and facilitate twisting between the quinoline rings. On the other hand, LUMO and LUMO+2 do not have such a node and the corresponding excited states adopt more planar conformations. In M2biQ, the nonradiative decay of excited singlets is followed by the blue $S_1 \rightarrow S_0$ emission. The calculated emission wavelength of 456 nm differs by only 12 nm from the observed emission.

The calculations also show that, in the S_1 excited state, the electron density asymmetrically shifts away from the methoxy groups to the nitrogen and carbon atoms in the bay area. Upon nitrogen protonation or metal coordination, the shape of the LUMO does not change significantly, while the HOMO becomes increasingly more localized in one of the halves of the ligand (see p S171). The smaller the cation, the shorter the N–cation distance, and the greater the loss of HOMO delocalization. This decreases the HOMO–LUMO gap and leads to increasingly red-shifted emissions in the progression $K^+ \rightarrow Sr^{2+} \rightarrow Ca^{2+} \rightarrow Cd^{2+} \rightarrow Zn^{2+} \rightarrow H^+$. This trend is clearly demonstrated by the strong correlations of the metal–nitrogen distances and ionic radii[83] with the emission wavelengths (Figure 5). DFT studies involving 8-HQ and its chelates found similar correlations.[84]

It is noteworthy that the $S_1 \rightarrow S_0$ emission is almost exclusively dominated by the LUMO–HOMO transitions with no significant contributions from other orbital pairs. This results in a strong correlation between the HOMO–LUMO and S_1–S_0 energy gaps as shown in Figure 6.

In conclusion, M2biQ is a novel versatile fluorophore whose emission wavelength is tunable throughout the visible spectrum by binding cations. In MeCN, the free M2biQ

https://dx.doi.org/10.1021/jacs.0c08182
J. Am. Chem. Soc. 2020, 142, 20306−20312

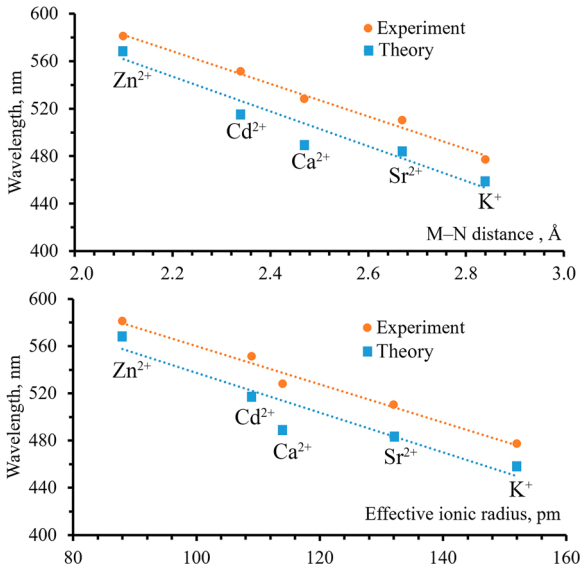

Figure 5. Correlations of ionic radii and metal−nitrogen distances with experimentally measured and computed emission wavelengths in 1:1 M2biQ complexes.

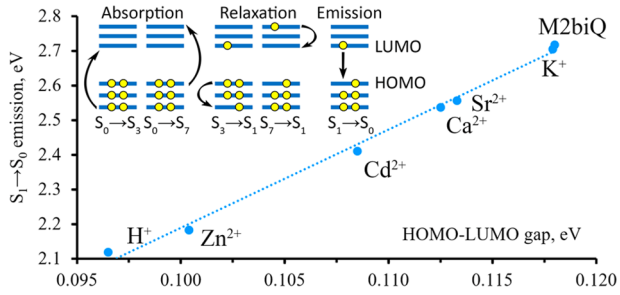

Figure 6. Proposed mechanism for M2biQ absorption and emission (inset) and correlation between calculated HOMO−LUMO gaps and energy differences between S_1 and S_0 states at the S_1 minimum.

fluorophore, its metal complexes, and the monoprotonated form span the spectral range from 468 to 690 nm with unusually large Stokes shifts up to ∼300 nm (∼12 000 cm^{-1}). The emission colors of all studied compounds remain qualitatively the same in the solid state. Single crystal X-ray structures show that, for 1:1 complexes, the smaller the cation, the shorter the N−cation bond, and the greater the planarization, consistent with the bathochromic shift of emission. These concepts can be useful for the design of chemosensors consisting of ligands containing chromophores that geometrically respond to binding of various cations. While cation binding lowers the energies of both HOMO and LUMO, the stabilization of the HOMO is less efficient due to decreasing delocalization in the progression $K^+ \rightarrow Sr^{2+} \rightarrow Ca^{2+} \rightarrow Cd^{2+} \rightarrow Zn^{2+} \rightarrow H^+$. This reduces the HOMO−LUMO gap and the S_1−S_0 gap and leads to an exceptional red shift in the emission spectra. Thus, M2biQ-based materials with nearly universal emission tunability may be used as fluorescent chemosensors and luminophores in various applications, including OLEDs. Such materials can be fabricated by simply doping an M2biQ-containing matrix with appropriate salts and/or acids.

■ ASSOCIATED CONTENT

Supporting Information

The Supporting Information is available free of charge at https://pubs.acs.org/doi/10.1021/jacs.0c08182.

Synthesis procedures and characterization data, titration experiments, emission and excitation spectra, quantum yields, lifetimes, electronic structure calculations, and crystallographic data of key substances (PDF)

Crystal structure data for M2biQ, M2biQ + Ca perchlorate, M2biQ + Zn perchlorate, M2biQ + $HClO_4$ + water, M2biQ$_2$ Zn perchlorate, and M2biQ + $HClO_4$ anhydrous (ZIP)

■ AUTHOR INFORMATION

Corresponding Author

Andrés Zavaleta − *Department of Chemistry, University of Nevada, Reno, Nevada 89557-0216, United States;* orcid.org/0000-0001-7995-1869; Email: Andres.Zavaleta@ucc.edu

Authors

Aleksandr O. Lykhin − *Department of Chemistry, University of Nevada, Reno, Nevada 89557-0216, United States;* orcid.org/0000-0002-9366-5866

Jorge H. S. K. Monteiro − *Department of Chemistry, University of Nevada, Reno, Nevada 89557-0216, United States;* orcid.org/0000-0002-9622-3537

Shoto Uchida − *Department of Chemistry, University of Nevada, Reno, Nevada 89557-0216, United States*

Thomas W. Bell − *Department of Chemistry, University of Nevada, Reno, Nevada 89557-0216, United States;* orcid.org/0000-0003-4986-9180

Ana de Bettencourt-Dias − *Department of Chemistry, University of Nevada, Reno, Nevada 89557-0216, United States;* orcid.org/0000-0001-5162-2393

Sergey A. Varganov − *Department of Chemistry, University of Nevada, Reno, Nevada 89557-0216, United States;* orcid.org/0000-0001-8301-3891

Judith Gallucci − *Department of Chemistry and Biochemistry, Ohio State University, Columbus, Ohio 43210, United States*

Complete contact information is available at: https://pubs.acs.org/10.1021/jacs.0c08182

Notes

The authors declare the following competing financial interest(s): The corresponding author declares a competing financial interest. Details accompany this paper.

■ ACKNOWLEDGMENTS

A.Z. was funded by the Ohio State University (OSU—Columbus and —Lima). S.A.V. is supported by the National Science Foundation (NSF) through a CAREER Award (CHE-1654547). A.d.B.D. is grateful to the NSF for funding (CHE-1800392). A.Z. is thankful to Dr. Chunhua Yuan (OSU) for collecting the high field NMR spectra and to Prof. Dennis Bong (OSU) for access to his spectrometers for preliminary luminescence studies. Dr. Jeanette A. Krause (University of Cincinnati) collected the crystallographic data for the Ca^{2+} complex through the SCrALS (Service Crystallography at Advanced Light Source) Program at Beamline 11.3.1 at the Advanced Light Source (ALS), Lawrence Berkeley National Laboratory. Dr. Brendan Twamley (Trinity University) is

thanked for completing the refinement of the crystal structure of the 2:1 Zn^{2+} complex.

REFERENCES

(1) Xia, Y.; Chen, S.; Ni, X. L. White Light Emission from Cucurbituril-Based Host-Guest Interaction in the Solid State: New Function of the Macrocyclic Host. *ACS Appl. Mater. Interfaces* **2018**, *10*, 13048−13052.
(2) Li, M.; Yuan, Y.; Chen, Y. Acid-Induced Multicolor Fluorescence of Pyridazine Derivative. *ACS Appl. Mater. Interfaces* **2018**, *10*, 1237−1243.
(3) Chirdon, D. N.; Transue, W. J.; Kagalwala, H. N.; Kaur, A.; Maurer, A. B.; Pintauer, T.; Bernhard, S. [Ir(N̂N̂N)(Ĉ N)L]+: A New Family of Luminophores Combining Tunability and Enhanced Photostability. *Inorg. Chem.* **2014**, *53*, 1487−1499.
(4) Xu, H.; Chen, R.; Sun, Q.; Lai, W.; Su, Q.; Huang, W.; Liu, X. Recent Progress in Metal-Organic Complexes for Optoelectronic Applications. *Chem. Soc. Rev.* **2014**, *43*, 3259−3302.
(5) Dong, B.; Wang, M.; Xu, C.; Feng, Q.; Wang, Y. Tuning Solid-State Fluorescence of a Twisted π-Conjugated Molecule by Regulating the Arrangement of Anthracene Fluorophores. *Cryst. Growth Des.* **2012**, *12*, 5986−5993.
(6) Pi, X.; Liptak, R.; Ligman, R.; Kortshagen, U.; Campbell, S. A. Full Spectrum Emission and Hybrid OLEDs from Silicon Nanoparticles. *In 4th IEEE International Conference on Group IV Photonics* **2007**, 249−251.
(7) Kokado, K.; Chujo, Y. Multicolor Tuning of Aggregation-Induced Emission through Substituent Variation of Diphenyl-o-Carborane. *J. Org. Chem.* **2011**, *76*, 316−319.
(8) Montes, V. A.; Pohl, R.; Shinar, J.; Anzenbacher, P. Effective Manipulation of the Electronic Effects and Its Influence on the Emission of 5-Substituted Tris(8-Quinolinolate) Aluminum(III) Complexes. *Chem. - Eur. J.* **2006**, *12*, 4523−4535.
(9) Qin, Y.; Kiburu, I.; Shah, S.; Jäkle, F. Luminescence Tuning of Organoboron Quinolates through Substituent Variation at the 5-Position of the Quinolato Moiety. *Org. Lett.* **2006**, *8*, 5227−5230.
(10) Kwon, J. E.; Park, S.; Park, S. Y. Realizing Molecular Pixel System for Full-Color Fluorescence Reproduction: RGB-Emitting Molecular Mixture Free from Energy Transfer Crosstalk. *J. Am. Chem. Soc.* **2013**, *135*, 11239−11246.
(11) Zhu, J.-L.; Xu, L.; Ren, Y.-Y.; Zhang, Y.; Liu, X.; Yin, G.-Q.; Sun, B.; Cao, X.; Chen, Z.; Zhao, X.-L.; Tan, H.; Chen, J.; Li, X.; Yang, H.-B. Switchable organoplatinum metallacycles with high quantum yields and tunable fluorescence wavelengths. *Nat. Commun.* **2019**, *10*, 4285.
(12) Chang, X.; Zhou, Z.; Shang, C.; Wang, G.; Wang, Z.; Qi, Y.; Li, Z.-Y.; Wang Cao, L. H.; Li, X.; Fang, Y.; Stang, P. J. Coordination-Driven Self-Assembled Metallacycles Incorporating Pyrene: Fluorescence Mutability, Tunability, and Aromatic Amine Sensing. *J. Am. Chem. Soc.* **2019**, *141*, 1757−1765.
(13) Hotta, S.; Yamao, T.; Bisri, S. Z.; Takenobuc, T.; Iwasade, Y. Organic single-crystal light-emitting field-effect Transistors. *J. Mater. Chem. C* **2014**, *2*, 965−980.
(14) Sun, Y.; Yao, Y.; Wang, H.; Fu, W.; Chen, C.; Saha, M. L.; Zhang, M.; Datta, S.; Zhou, Z.; Yu, H.; Li, X.; Stang, P. J. Self-Assembly of Metallacages into Multidimensional Suprastructures with Tunable Emissions. *J. Am. Chem. Soc.* **2018**, *140* (40), 12819−12828.
(15) Belyaev, A.; Cheng, Y.-H.; Liu, Z.-Y.; Karttunen, A. J.; Chou, P.-T.; Koshevoy, I. O. A Facile Molecular Machine: Optically Triggered Counterion Migration via Charge Transfer of Linear D-π-A Phosphonium Fluorophores. *Angew. Chem., Int. Ed.* **2019**, *58*, 13456−13465.
(16) Medintz, I. L.; Uyeda, H. T.; Goldman, E. R.; Mattoussi, H. Quantum Dot Bioconjugates for Imaging, Labelling and Sensing. *Nat. Mater.* **2005**, *4*, 435−446.
(17) Hildebrandt, N.; Spillmann, C. M.; Algar, W. R.; Pons, T.; Stewart, M. H.; Oh, E.; Susumu, K.; Díaz, S. A.; Delehanty, J. B.; Medintz, I. L. Energy Transfer with Semiconductor Quantum Dot Bioconjugates: A Versatile Platform for Biosensing, Energy Harvesting, and Other Developing Applications. *Chem. Rev.* **2017**, *117*, 536−711.
(18) Sreenath, K.; Clark, R. J.; Zhu, L. Tricolor Emission of a Fluorescent Heteroditopic Ligand over a Concentration Gradient of Zinc(II) Ions. *J. Org. Chem.* **2012**, *77*, 8268−8279.
(19) Shiraishi, Y.; Ichimura, C.; Sumiya, S.; Hirai, T. Multicolor Fluorescence of a Styrylquinoline Dye Tuned by Metal Cations. *Chem. - Eur. J.* **2011**, *17*, 8324−8332.
(20) Zucchero, A. A.; McGrier, P. J.; Bunz, U. H. Cross-Conjugated Cruciform Fluorophores. *Acc. Chem. Res.* **2010**, *43*, 397−408.
(21) Younes, A. H.; Zhang, L.; Clark, R. J.; Zhu, L. Fluorescence of 5-Arylvinyl-5′-Methyl-2,2′-Bipyridyl Ligands and Their Zinc Complexes. *J. Org. Chem.* **2009**, *74*, 8761−8772.
(22) Wang, Z.; Palacios, M. A.; Anzenbacher, P. Fluorescence Sensor Array for Metal Ion Detection Based on Various Coordination Chemistries: General Performance and Potential Application. *Anal. Chem.* **2008**, *80*, 7451−7459.
(23) Palacios, M. A.; Wang, Z.; Montes, V. A.; Zyryanov, G. V.; Hausch, B. J.; Jursíková, K.; Anzenbacher, P. Hydroxyquinolines with Extended Fluorophores: Arrays for Turn-on and Ratiometric Sensing of Cations. *Chem. Commun.* **2007**, *7345*, 3708−3710.
(24) Knapton, D.; Burnworth, M.; Rowan, S. J.; Weder, C. Fluorescent Organometallic Sensors for the Detection of Chemical-Warfare-Agent Mimics. *Angew. Chem., Int. Ed.* **2006**, *45*, 5825−5829.
(25) Joshi, H. S.; Jamshidi, R.; Tor, Y. Conjugated 1,10-Phenanthrolines as Tunable Fluorophores. *Angew. Chem., Int. Ed.* **1999**, *38*, 2721−2725.
(26) Li, W.; Zhang, Y. M.; Zhang, T.; Zhang, W.; Li, M.; Zhang, S. X. A. Tunable RGB Luminescence of a Single Molecule with High Quantum Yields through a Rational Design. *J. Mater. Chem. C* **2016**, *4*, 1527−1532.
(27) Ahn, H.; Hong, J.; Kim, S. Y.; Choi, I.; Park, M. J. A pH-Responsive Molecular Switch with Tricolor Luminescence. *ACS Appl. Mater. Interfaces* **2015**, *7*, 704−712.
(28) Zhang, Q. W.; Li, D.; Li, X.; White, P. B.; Mecinović, J.; Ma, X.; Ågren, H.; Nolte, R. J. M.; Tian, H. Multicolor Photoluminescence Including White-Light Emission by a Single Host-Guest Complex. *J. Am. Chem. Soc.* **2016**, *138*, 13541−13550.
(29) Matsunaga, Y.; Yang, J. S. Multicolor Fluorescence Writing Based on Host-Guest Interactions and Force-Induced Fluorescence-Color Memory. *Angew. Chem., Int. Ed.* **2015**, *54*, 7985−7989.
(30) Lavigne, J. J.; Anslyn, E. V. Sensing a Paradigm Shift in the Field of Molecular Recognition: From Selective to Differential Receptors. *Angew. Chem., Int. Ed.* **2001**, *40*, 3118−3130.
(31) Lei, Y.; Dai, W.; Guan, J.; Guo, S.; Ren, F.; Zhou, Y.; Shi, J.; Tong, B.; Cai, Z.; Zheng, J.; Dong, Y. Wide-Range Color-Tunable Ultralong Organic Phosphorescence Materials for Printable and Writable Security Inks. *Angew. Chem.* **2020**, *132*, 16188−16194.
(32) Tian, H.; Zhang, T.; Ma, X.; Wu, H.; Zhu, L.; Zhao, Y. Molecular Engineering for Metal-free Amorphous Room-temperature Phosphorescent Materials. *Angew. Chem., Int. Ed.* **2020**, *59*, 11206−11216.
(33) Wang, Q.; Zhang, Q.; Zhang, Q.-W.; Li, X.; Zhao, C.-X.; Xu, T.-Y.; Qu, D.-H; Tian, H. Color-tunable single-fluorophore supramolecular system with assembly-encoded emission. *Nat. Commun.* **2020**, *11*, 158.
(34) Ma, X.; Wang, J.; Tian, H. Assembling-Induced Emission: An Efficient Approach for Amorphous Metal-Free Organic Emitting Materials with Room-Temperature Phosphorescence. *Acc. Chem. Res.* **2019**, *52*, 738−748.
(35) Zhang, M.; Yin, S.; Zhang, J.; Zhou, Z.; Saha, M. L.; Lu, C.; Stang, P. J. Metallacycle-cored supramolecular assemblies with tunable fluorescence including white-light emission. *Proc. Natl. Acad. Sci. U. S. A.* **2017**, *114*, 3044−3049.
(36) Kong, F. K.-W.; Chan, A. K.-W.; Ng, M.; Low, K.-H.; Yam, V. W.-W. Construction of Discrete Pentanuclear Platinum(II) Stacks with Extended Metal-Metal Interactions by Using Phosphorescent Platinum(II) Tweezers. *Angew. Chem., Int. Ed.* **2017**, *56*, 15103−15107.

https://dx.doi.org/10.1021/jacs.0c08182
J. Am. Chem. Soc. 2020, 142, 20306−20312

(37) Ni, X.-L.; Chen, S.; Yang, Y.; Tao, Z. A Facile Cucurbit[8]uril-Based Supramolecular Approach to Fabricate Tunable Luminescent Materials in Aqueous Solution. *J. Am. Chem. Soc.* **2016**, *138*, 6177−6183.
(38) Bouchouicha, H.; Panczer, G.; de Ligny, D.; Guyot, Y.; Ternane, R. Luminescent Properties of Eu-Doped Calcium Aluminosilicate Glass-Ceramics: A Potential Tunable Luminophore. *Opt. Mater. (Amsterdam, Neth.)* **2018**, *85*, 41−47.
(39) Zhang, C.; Yang, L.; Zhao, J.; Liu, B.; Han, M. Y.; Zhang, Z. White-Light Emission from an Integrated Upconversion Nanostructure: Toward Multicolor Displays Modulated by Laser Power. *Angew. Chem., Int. Ed.* **2015**, *54*, 11531−11535.
(40) Yuan, C.; Saito, S.; Camacho, C.; Irle, S.; Hisaki, I.; Yamaguchi, S. A π-Conjugated System with Flexibility and Rigidity That Shows Environment-Dependent RGB Luminescence. *J. Am. Chem. Soc.* **2013**, *135*, 8842−8845.
(41) Suzuki, S.; Sasaki, S.; Sairi, A. S.; Iwai, R.; Tang, B. Z.; Konishi, G.-i. Principles of Aggregation-Induced Emission: Design of Deactivation Pathways for Advanced AIEgens and Applications. *Angew. Chem., Int. Ed.* **2020**, *59*, 9856−9867.
(42) Zheng, K.; Ni, F.; Chen, Z.; Zhong, C.; Yang, C. Polymorph-Dependent Thermally Activated Delayed Fluorescence Emitters: Understanding TADF from a Perspective of Aggregation State. *Angew. Chem., Int. Ed.* **2020**, *59*, 9972−9976.
(43) Wurthner, F. Aggregation-Induced Emission (AIE): A historical Perspective. *Angew. Chem., Int. Ed.* **2020**, *59*, 14192−14196.
(44) Huang, B.; Chen, W.-C.; Li, Z.; Zhang, J.; Zhao, W.; Feng, Y.; Tang, B.-Z.; Lee, C.-S. Manipulation of Molecular Aggregation States to Realize Polymorphism, AIE, ML, and TADF in a Single Molecule. *Angew. Chem., Int. Ed.* **2018**, *57*, 12473−12477.
(45) Feng, H.-T.; Yuan, Y.-X.; Xiong, J.-B.; Zheng, Y.-S.; Tang, B. Z. Macrocycles and Cages Based on Tetraphenylethylene with Aggregation-induced Emission Effect. *Chem. Soc. Rev.* **2018**, *47*, 7452−7476.
(46) Chen, Y.; Zhang, W.; Zhao, Z.; Cai, Y.; Gong, J.; Kwok, R. T. K.; Lam, J. W. Y.; Sung, H. H. Y.; Williams, I. D.; Tang, B. Z. An Easily Accessible Ionic Aggregation-induced Emission Luminogen with Hydrogen Bonding Switchable Emission and Wash-free Imaging Ability. *Angew. Chem.* **2018**, *130*, 5105−5109.
(47) Mukherjee, S.; Thilagar, P. Stimuli and Shape responsive 'Boron-Containing' Luminescent Organic Materials. *J. Mater. Chem. C* **2016**, *4*, 2647−2662.
(48) Yan, X.; Cook, T. R.; Wang, P.; Huang, F.; Stang, P. J. Highly Emissive Platinum(II) Metallacages. *Nat. Chem.* **2015**, *7*, 342−348.
(49) Li, Y.; Lei, Y.; Dong, L.; Zhang, L.; Zhi, J.; Shi, J.; Tong, B.; Dong, Y. 1,2,5-Triphenylpyrrole Derivatives with Dual Intense Photoluminescence in Both Solution and the Solid State: Solvatochromism and Polymorphic Luminescence Properties. *Chem. - Eur. J.* **2018**, *25*, 573−581.
(50) Mori, T.; Yoshigoe, Y.; Kuninobu, Y. Control of Multicolor and White Emissions by Tuning Equilibrium Between Fluorophores, Lewis Acids, and Their Complexes Using Polymers. *Angew. Chem., Int. Ed.* **2019**, *58*, 14457−14461.
(51) Furue, R.; Nishimoto, T.; Park, I. S.; Lee, J.; Yasuda, T. Aggregation-Induced Delayed Fluorescence Based on Donor/Acceptor-Tethered Janus Carborane Triads: Unique Photophysical Properties of Nondoped OLEDs. *Angew. Chem., Int. Ed.* **2016**, *55*, 7171−7175.
(52) Lane, S.; Vagin, S.; Wang, H.; Heinz, W. R.; Morrish, W.; Zhao, Y.; Rieger, B.; Meldrum, A. Wide-gamut Lasing From A Single Organic Chromophore. *Light: Sci. Appl.* **2018**, *7*, 101.
(53) Hendon, C. H.; Walsh, A.; Akiyama, N.; Konno, Y.; Kajiwara, T.; Ito, T.; Kitagawa, H.; Sakai, K. One-dimensional Magnus-type platinum double salts. *Nat. Commun.* **2016**, *7*, 11950.
(54) Naren, G.; Hsu, C.-W.; Li, S.; Morimoto, M.; Tang, S.; Hernando, J.; Guirado, G.; Irie, M.; Raymo, F. M.; Sundén, H.; Andréasson, J. An all-photonic full color RGB system based on molecular photoswitches. *Nat. Commun.* **2019**, *10*, 3996.
(55) Bälter, M.; Li, S.; Morimoto, M.; Tang, S.; Hernando, J.; Guirado, G.; Irie, M.; Raymo, F. M.; Andréasson, J. Emission color tuning and white-light generation based on photochromic control of energy transfer reactions in polymer micelles. *Chem. Sci.* **2016**, *7*, 5867−5871.
(56) Hiblot, J.; Yu, Q.; Sabbadini, M. D. B.; Reymond, L.; Xue, L.; Schena, A.; Sallin, O.; Hill, N.; Griss, R.; Johnsson, K. Luciferases with Tunable Emission Wavelengths. *Angew. Chem., Int. Ed.* **2017**, *56*, 14556−14560.
(57) Gu, J.; Shi, H.; Bian, L.; Gu, M.; Ling, K.; Wang, X.; Ma, H.; Cai, S.; Ning, W.; Fu, L.; Wang, H.; Wang, S.; Gao, Y.; Yao, W.; Huo, F.; Tao, Y.; An, Z.; Liu, X.; Huang, W. Colour-tunable ultra-long organic phosphorescence of a single-component molecular crystal. *Nat. Photonics* **2019**, *13*, 406−411.
(58) Zheng, S.; Zhu, T.; Wang, Y.; Yang, T.; Yuan, W. Z. Accessing Tunable Afterglows from Highly Twisted Nonaromatic Organic AIEgens via Effective Through-Space Conjugation. *Angew. Chem., Int. Ed.* **2020**, *59*, 10018−10022.
(59) Zavaleta Fernández de Córdova, Andrés. Luminescent Polydentate Polycyclic Compounds for Metal Ions. United States Patent 10,633,586 B1. April 28, 2020.
(60) Hu, Y. Z.; Zhang, G.; Thummel, R. P. Friedländer Approach for the Incorporation of 6-Bromoquinoline into Novel Chelating Ligands. *Org. Lett.* **2003**, *5*, 2251−2253.
(61) Tröger, J.; Dunker, E. 2-Amino-3-methoxybenzaldehyd und einige Derivate desselben. *J. Prakt. Chem.* **1925**, *111*, 207−216.
(62) Chen, C. H.; Shi, J. Metal Chelates as Emitting Materials for Organic Electroluminescence. *Coord. Chem. Rev.* **1998**, *171*, 161−174.
(63) Ren, T.-B.; Xu, W.; Zhang, W.; Zhang, X.-X.; Wang, Z.-Y.; Xiang, Z.; Yuan, L.; Zhang, X.-B. A General Method To Increase Stokes Shift by Introducing Alternating Vibronic Structures. *J. Am. Chem. Soc.* **2018**, *140*, 7716−7722.
(64) Butkevich, A. N.; Lukinavičius, G.; D'Este, E.; Hell, S. W. Cell-Permeant Large Stokes Shift Dyes for Transfection-Free Multicolor Nanoscopy. *J. Am. Chem. Soc.* **2017**, *139*, 12378−12381.
(65) Gans, P.; Sabatini, A.; Vacca, A. Investigation of equilibria in solution. Determination of equilibrium constants with the HYPERQUAD suite of programs. *Talanta* **1996**, *43*, 1739−1753.
(66) Alderighi, L.; Gans, P.; Ienco, A.; Peters, D.; Sabatini, A.; Vacca, A. Hyperquad simulation and speciation (HySS): a utility program for the investigation of equilibria involving soluble and partially soluble species. *Coord. Chem. Rev.* **1999**, *184*, 311−318.
(67) Li, W.; Huang, Q.; Mao, Z.; Zhao, J.; Wu, H.; Chen, J.; Yang, Z.; Li, Y.; Yang, Z.; Zhang, Y.; Aldred, M. P.; Chi, Z. Selective Expression of Chromophores in a Single Molecule: Soft Organic Crystals Exhibiting Full-Colour Tunability and Dynamic Triplet-Exciton Behaviours. *Angew. Chem., Int. Ed.* **2020**, *59*, 3739−3745.
(68) Moya, S. A.; Guerrero, J.; Rodriguez-Nieto, F. J.; Wolcan, E.; Féliz, M. R.; Baggio, R. F.; Garland, M. T. Influence of the 4-Substituted Pyridine Ligand L' on both the Conformation and Spectroscopic Properties of the (2,2'-Biquinoline*kN*1, k*N*1')-tricarbonyl(pyridine-k*N*1)rhenium(1+) Complex ([Re(CO)3-(bqui)-(py)]+) and Its Derivatives [Re(CO)3(L)(L')]+ (L = 2,2'-Biquinoline and 3,3′-(Ethane-1,2-diyl)-2,2'-biquinoline). *Helv. Chim. Acta* **2005**, *88*, 2842−2860.
(69) Melhuish, W. H. Quantum Efficiencies of Fluorescence of Organic Substances: Effect of Solvent and Concentration of the Fluorescent Solute. *J. Phys. Chem.* **1961**, *65*, 229−235.
(70) Brouwer, A. M. Standards for photoluminescence quantum yield measurements in solution (IUPAC Technical Report). *Pure Appl. Chem.* **2011**, *83*, 2213−2228.
(71) Nakamaru, K. Synthesis, Luminescence Quantum Yields, and Lifetimes of Trischelated Ruthenium(II) Mixed-ligand Complexes Including 3,3′-Dimethyl-2,2′-bipyridyl. *Bull. Chem. Soc. Jpn.* **1982**, *55*, 2697−2707.
(72) Zhang, H.; Wang, Q.-L.; Jiang, Y.-B. 8-Methoxyquinoline based Turn-on Metal Fluoroionophores. *Tetrahedron Lett.* **2007**, *48*, 3959−3962.

https://dx.doi.org/10.1021/jacs.0c08182
J. Am. Chem. Soc. 2020, 142, 20306−20312

(73) Mello, J. V.; Finney, N. S. Dual-Signaling Fluorescent Chemosensors Based on Conformational Restriction and Induced Charge Transfer. *Angew. Chem., Int. Ed.* **2001**, *40*, 1536−1538.
(74) Achelle, S.; Rodríguez López, J.; Katan, C.; Le Guen, F. R. *J. Phys. Chem. C* **2016**, *120* (47), 26986−26995.
(75) Sohna, J.-E.; Jaumier, P.; Fages, F. Zinc(II)-driven Fluorescence Quenching of a Pyrene-labelled Bis-2,2′-bipyridine Ligand. *J. Chem. Res., Synop.* **1999**, 134−135.
(76) Rodriguez, A. L.; Peron, G.; Duprat, C.; Vallier, M.; Fouquet, E.; Fages, F. The Use of a Monoorganotin Derivative of Pyrene in the Palladium(0)-catalized Synthesis of a New Metal-Cation Complexing Molecule Displaying Excited State Charge Transfer Properties. *Tetrahedron Lett.* **1998**, *39*, 1179−1182.
(77) Bardez, E.; Devol, I.; Larrey, B.; Valeur, B. Excited-State Processes in 8-Hydroxyquinoline: Photoinduced Tautamerization and Solvation Effects. *J. Phys. Chem. B* **1997**, *101*, 7786−7793.
(78) Farruggia, G.; Iotti, S.; Prodi, L.; Montalti, M.; Zaccheroni, N.; Savage, P. B.; Trapani, V.; Sale, P.; Wolf, F. I. 8-Hydroxyquinoline Derivatives as Fluorescent Sensors for Magnesium in Living Cells. *J. Am. Chem. Soc.* **2006**, *128*, 344−350.
(79) Soloman, S. *Sensors and Control Systems in Manufacturing*, 2nd ed.; McGraw-Hill: New York, 2010; pp 10−25.
(80) Tang, H.; Meng, G.; Chen, Z.; Wang, K.; Zhou, Q.; Wang, Z. Warm White Light-Emitting Diodes Based on a Novel Orange Cationic Iridium(III) Complex. *Materials* **2017**, *10*, 657.
(81) Haberhauer, G.; Gleiter, R.; Burkhart, C. Planarized Intramolecular Charge Transfer: A Concept for Fluorophores with both Large Stokes Shifts and High Fluorescence Quantum Yields. *Chem. - Eur. J.* **2016**, *22*, 971−978.
(82) Chen, Y.; Zhao, J.; Guo, H.; Xie, L. Geometry Relaxation-Induced Large Stokes Shift in Red-Emitting Borondipyrromethenes (BODIPY) and Applications in Fluorescent Thiol Probes. *J. Org. Chem.* **2012**, *77*, 2192−2206.
(83) Shannon, R. D. Revised Effective Ionic Radii and Systematic Studies of Interatomic Distances in Halides and Chalcogenides. *Acta Crystallogr., Sect. A: Cryst. Phys., Diffr., Theor. Gen. Crystallogr.* **1976**, *A32*, 751−767.
(84) Núñez-Zarur, F.; Vivas-Reyes, R. Ab initio study of luminescent substituted 8-hydroxyquinoline metal complexes with application in organic light emitting diodes. *J. Mol. Struct.: THEOCHEM* **2008**, *850*, 127−134.

https://dx.doi.org/10.1021/jacs.0c08182
J. Am. Chem. Soc. 2020, 142, 20306−20312